Mitigating flood risk and environmental change in show caves: Key challenges in the management of the Las Güixas cave (Pyrenees, Spain)

Author(s):
Giménez, Reyes; Moreno, Ana; Luetscher, Marc; Ezquerro, Lope; Delgado-Huertas, Antonio; Benito, Gerardo; Bartolomé, Miguel

Publication date:
2024-11

Permanent link:
https://doi.org/10.3929/ethz-b-000693768

Originally published in:
Journal of Environmental Management 370, https://doi.org/10.1016/j.jenvman.2024.122285

Journal of Environmental Management 370 (2024) 122285

Contents lists available at ScienceDirect

Journal of Environmental Management

journal homepage: www.elsevier.com/locate/jenvman

Research article

Mitigating flood risk and environmental change in show caves: Key challenges in the management of the Las Güixas cave (Pyrenees, Spain)

Reyes Giménez [a], Ana Moreno [a,*], Marc Luetscher [b], Lope Ezquerro [c], Antonio Delgado-Huertas [d], Gerardo Benito [e], Miguel Bartolomé [b,e,f]

[a] Instituto Pirenaico de Ecología, IPE–CSIC, 50059, Zaragoza, Spain
[b] Swiss Institute for Speleology and Karst Studies (SISKA), 2300, La Chaux-de-Fonds, Switzerland
[c] Departamento de Ciencias de la Tierra, Facultad de Ciencias Geológicas, Universidad Complutense de Madrid, 28040, Madrid, Spain
[d] Laboratorio de Biogeoquímica de Isótopos Estables, IACT-CSIC, 18100, Armilla Granada, Spain
[e] Museo Nacional de Ciencias Naturales, MNCN – CSIC, 28006, Madrid, Spain
[f] Geological Institute, NO G59, Department of Earth Sciences, ETH, 8092, Zurich, Switzerland

ARTICLE INFO

Handling editor: Lixiao Zhang

Keywords:
Cave monitoring
Cave climatology
Cave ventilation
CO_2 sources
Flooding cave
Flood hydrographs

ABSTRACT

A successful management of a show cave requires knowledge of cave dynamics and the main risk factors. Show caves close to the water table are prone to sporadic flooding, which can threaten visitor safety and result in severe economic losses. Las Güixas cave, located in the Collarada Massif (Pyrenees - Spain), is representative of a show cave close to the water table that is exposed to energetic flash floods. We conducted a five-year comprehensive cave monitoring study including air temperature, relative humidity, CO_2 concentration and water level. Additionally, we measured outside temperature and precipitation. Air temperature variations and ventilation dynamics occurring in most of the cave are controlled by the outside temperature due to entrances at different elevations, except in a non-ventilated area showing more stable hygrothermal characteristics and higher summer values of CO_2 concentration. The study also identifies distinct CO_2 sources related to the degassing of water and visitors' breathing. Monitoring data show that the rapid degassing of cave water during flooding may increase subsurface CO_2 concentrations to levels well above the exposure limits. However, the strong ventilation observed inside the cave rapidly removes CO_2 peaks produced by flooding and limits the anthropic CO_2 rise to ~100 ppm. Hydrograph analysis revealed a response time of 8–12 h in the cave water levels to external rainfall/snowmelt events. Based on these results, a flood alarm system supports sustainable show cave management and the number of visitors is optimized according to the environmental conditions of the cave. This monitoring study has greatly contributed to our knowledge of cave dynamics, which can serve to improve flood risk management and increase the profitability of the show cave. Nonetheless, extreme floods remain a significant concern for potential economic losses in the future, considering current climate change scenarios. Hydrological studies together with a long-term monitoring will allow evaluating the impact of future changes in climate and environmental parameters.

1. Introduction

Caves are places with important natural and cultural heritage assets. Caves open to tourism, so-called show caves, provide an excellent opportunity to spread the knowledge and awareness of the underground system (Chiarini et al., 2022; Cigna and Forti, 2013). Nowadays, more than 1200 show caves worldwide receive more than 80 million visitors per year, thus representing an important economic resource (Chiarini et al., 2022; Cigna and Burri, 2000). In Spain, the first show caves were opened at the early 19th century. Their popularity increased during the second half of the 20th century in relation to the development of tourism focused on natural landscapes and heritage resources, being now a crucial part of the national/local economy (Rivas et al., 2004). The exploitation of a cave for tourism involves alterations in the cave environment and visitors influence has been evidenced through a rise in cave temperature, a decrease in the cave humidity, and/or increase in CO_2 concentration (Baker and Genty, 1998; Fernández-Cortés et al., 2006; Gázquez et al., 2016; Guirado et al., 2015; Lang et al., 2024). Changes in

* Corresponding author.
E-mail address: amoreno@ipe.csic.es (A. Moreno).

https://doi.org/10.1016/j.jenvman.2024.122285
Received 16 March 2024; Received in revised form 29 July 2024; Accepted 23 August 2024
Available online 9 September 2024

cave humidity, temperature and CO_2 contribution may affect carbonate dissolution and precipitation, altering chemical equilibrium and weathering, and even favoring speleothem corrosion (Baker and Genty, 1998; Fernandez-Cortes et al., 2011; Lang et al., 2024; Nicolas et al., 2017). The impact of tourism depends on the number of visitors, the average time visitors remain in the cave and the cave ventilation (Rivas et al., 2004). Besides, visitors may be exposed to potential risks inside a cave, such as the exposure to harmful gas concentrations levels. Cave monitoring, including air and water temperature, relative humidity, pressure, CO_2 and radon concentrations, allows identifying and evaluating tourism impacts and accurately defining the visitors' risk in a specific cave. The study of these parameters thus provides useful information about the cave's microclimate evolution and thermodynamics, supporting effective cave management (Bourges et al., 2006, 2020; Spötl et al., 2005).

The CO_2 concentration in the cave air is the parameter that deserves more attention, being a function of both production and ventilation processes. Under natural conditions, CO_2 in the cave atmosphere originates from several sources, such as soil respiration, biological productivity and oxidation of organic matter in the cave or even CO_2 from hypogene origin (Baldini, 2010; Troester and White, 1984). In show caves, visitors' breathing is also a source of CO_2 (Cigna, 1993; Constantin et al., 2021). Cave ventilation, driven by temperature-induced airflow, depends on cave morphology, the number of entrances and their position (Faimon et al., 2012; Mattey et al., 2021). Caves with multiple entrances can be strongly ventilated due to a stack effect with bidirectional airflows resulting in downward airflow and upward airflow ventilation modes with a transitional mode in between (Faimon et al., 2012). In terms of the energy fluxes with the external environment, caves with strong ventilation regimes are classified by Heaton (1986) as high-energy caves, similar to caves frequently flooded by rivers and subject to high-energy flows. High-energy caves are more prone to be disturbed by natural processes than by tourist activity (Cigna and Burri, 2000). Nonetheless, caves that are frequently flooded pose a risk that can only be addressed by knowledge of the hydrological dynamics, through an adequate cave monitoring. These karst systems have a non-linear response to rainfall, characterised by thresholds associated with hydrological bypasses that difficult evaluating the risk of flooding (Jeannin and Malard, 2018). An abrupt increase in water levels inside the caves, even in response to a gradual precipitation, threatens the lives of people present in the cave. Two examples are the 2018 rescue of children in Tham Luang cave, Thailand (Ahmed et al., 2021), and a rescue of cavers in Spain the same year (Bartolomé et al., 2023). Show caves located in the epiphreatic zone, therefore, require accurate flood hazard and risk assessment to ensure safe tourist activities and reduce economic losses.

There are very few show caves affected by floods in the Mediterranean region. To our knowledge, only two show caves in Spain suffer from periodic or occasional flooding along their entire tourist routes. Despite the associated risk for visitors, there are no studies on understanding the dynamics that generate floods in these caves and no strategies to aid in cave management. We present monitoring data from Las Güixas show cave, Central Pyrenees, located in the epiphreatic zone of the Collarada karst system. Importantly, very little was known about changes in the cave water level as a response to external rainfall previous to this study. The water level in the cave changes quickly, as in 1974, when an accident triggered by a sudden rise in the water level caused death of a diver during the exploration of the main siphon. Later, in 2012, an extreme flood (Acín et al., 2012; Serrano-Muela et al., 2013), caused the destruction of facilities in the tourist sector of the cave. This comprehensive monitoring includes the study of water level, drip water rate, CO_2 concentrations, temperature and relative humidity in several cave sectors, together with the number of visitors since 2017. No scientific studies on the Las Güixas cave dynamics have been conducted to date nor similar studies in other Pyrenean caves being show caves or not. The main objective of this study is to accurately describe variations in the environmental parameters and to improve our understanding of the current hydrological dynamics. This information is later used to assess the possible influence of the visitors on the cave dynamics and to propose some actions and investments for flood risk adaptation, increasing the profitability of the show cave.

2. Study site

2.1. Cave location and climate setting

Las Güixas show cave (LGSC henceforth) is located in the southern Central Western Pyrenees (NE of Spain) at the base of the Collarada Massif (975 m a.s.l.) next to the Aragon River and close to the Villanúa village (Fig. 1a). The cave develops in Eocene-aged carbonates of the Villanúa megabreccia and corresponds with one of the main springs of the Collarada system, a still not fully explored karstic system that drains an area of ~20 km^2.

The climate is transitional Mediterranean to Oceanic. The mean annual temperature (MAAT) is ~11 °C, and total precipitation is ~1100 mm. Most precipitation takes place between October and May, associated to Atlantic fronts. During summer, the Azores anticyclone prevents the entry of Atlantic storms while convective events are able to produce sudden and intense rainfall events. Spring and autumn are affected by both, alternating, dynamics and moisture sources, causing a changing and unstable rainy weather resulting in the largest amount of precipitation per event (Giménez et al., 2021).

LGSC has been continuously occupied at least since the Bronze Age (Lorenzo, 1992; Rodanés et al., 2016), and is easy accessible from Villanúa village through a historic passageway (*Camino de Santiago*, the Way of St. James). The cave was first opened for tourism in 1929 and closed during the Spanish Civil War (1936–1939), when light wiring was removed. It served as a prison for a time, after which the cave remained closed, with sporadic visits and access provided by the town council. A new lighting system and other facilities served to open the cave again to the tourism in 1996 until present. LGSC stays open for visitors the whole year and visits have doubled since 2012, exceeding 30,000 visitors today. Its income has tripled over the same period, making it the main economic asset of the village of Villanúa.

2.2. Cave morphology and hydrology

LGSC is a shallow cave (2–27 m bedrock) with ~1100 m development and ~67 m vertical extent. The cave is well decorated with speleothems (flowstones, flags, stalagmites and stalactites) and contains clastic deposits resulting from collapses and floods. The cave has three levels: i) the lower level (phreatic) is accessible only by diving techniques, and comprises two explored siphons and several galleries with an active stream (Fig. 1c); ii) the middle level (epi-phreatic) is open to tourism but hydrologically active during floods. This level has two cave entrances: the main tourist entrance (E1, 975 m a.s.l.), and a 6 m deep sinkhole (E2) connecting the surface to the cave (Fig. 1c). Finally, iii) the upper level comprises the highest galleries with two more entrances: E3 corresponding to a descending passage from the surface (1008 m a.s.l) and E4 (1017 m a.s.l) corresponding with an almost horizontal gallery.

The water in the LGSC flows through a small passage from the siphon 1 to the Aragón River (Fig. 1b c), where a spring drains most water of the system, ~6 m above the riverbed (Fig. 1b). The spring is active throughout the year, but it dries up completely during extreme droughts. The middle cave level connects with the permanently flooded lower level by a ramp (−15 m) ending in the siphon 1 (Fig. 1c). After rainfalls or during snowmelt, the water from the lower level ascends ~15 m reaching the middle touristic level that works as a trop-plein, forcing the cancellation of visiting tours. The water flows along this level and disappears through the west siphon, located close to the touristic entrance (Fig. 1c). The upper level is not anymore affected from the hydrological activity associated with floods, even though a narrow passage from the

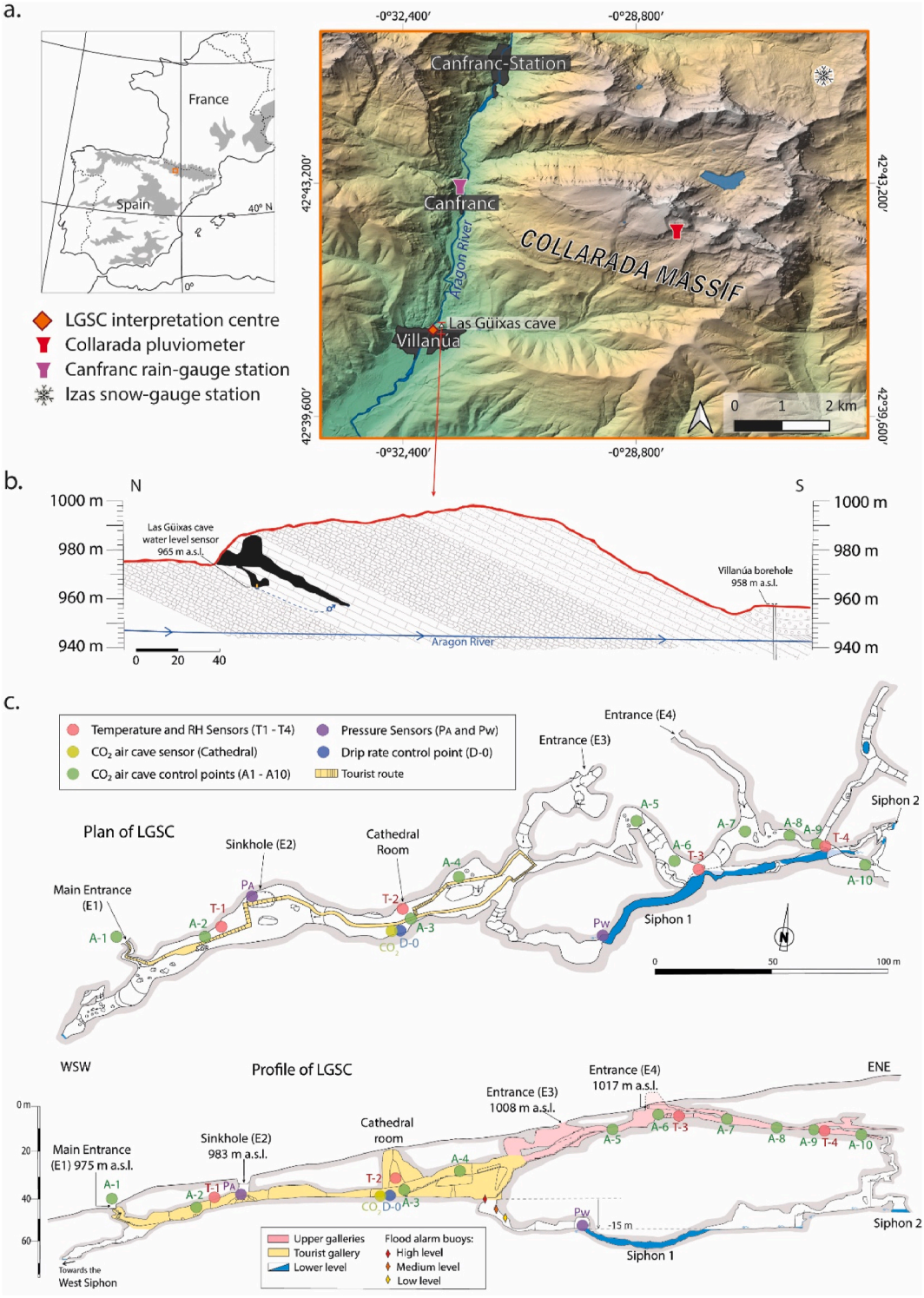

Fig. 1. **(a)** Situation of the Collarada Massif in the Pyrenees and location of Las Güixas cave in the Aragon Valley. **(b)** The north-south cross section shows a projection of the cave with the location of the water level sensor and the position of the piezometer of the Villanúa borehole with respect to the Aragon River. **(c)** Plan and profile of the cave with the location of sensors and control points. Sensors T1-T4 (red dots) measure temperature and RH and CO_2 air cave sensor (yellow dot) measure CO_2 concentration at the Cathedral room. Control points indicate where manual measure was carried out for CO_2 concentration (green dots numbered with A) and for drip rate (blue dot D-0). (For interpretation of the references to colour in this figure legend, the reader is referred to the Web version of this article.)

end of an upper gallery communicates directly with the lower level (Fig. 1c). Although, the cave has been explored by several teams of cavers, the phreatic galleries are less known due to the difficulty involved in their exploration. The longest exploration was carried out in 1991, when siphons 1 and 2 (Fig. 1c) were dived and it was located a third siphon that remains unexplored.

The exceptional rainfall in the headwaters of the Aragón River basin from the 19th to 21st October, 2012 (235 mm of rainfall at Canfranc) caused the complete flooding of the cave producing many damages inside. The entire tourist path remained several days under water,

handrails, power lines and other facilities were destroyed and the touristic entrance acted as a trop-plein. A new spring appeared ~125m above the cave and several damages were caused in the surroundings. As a result, a flood alarm was installed in the cave to warn of dangerous water levels during rainy days.

3. Methods

LGSC was monitored between July 2017 and June 2022, including instrumental tracking of environmental and hydrological parameters together with manual measurements and sampling. Information on the number of people in the cave per day has been recovered from the Visitor Centre database.

3.1. Morphological data

Mapping based on the location and elevation of the main geomorphological features (e.g. siphons, galleries, entrances) and monitoring sensors positioning, was conducted using a DistoX2 Leica (x310) modified with an electronic base plate to measure the direction and dip between selected points in the cave (Heeb, 2014). The data were processed using VisualTopo software (http://vtopo.free.fr).

3.2. Meteorological data

Air temperature and precipitation amount at 15-min intervals were obtained from a gauging station of the Ebro Water Administration (Confederación Hidrográfica del Ebro; CHE) in the village of Canfranc (4 km north of the cave, Fig. 1). Snow depth was obtained from the CHE station at Izas Valley (2086 m a.s.l.), 10 km north of the cave. A pluviometer was installed near to the LGSC interpretation centre, where rainfall amount and rainfall temperature were measured manually after each event >1 mm (Giménez et al., 2021 and new data). A second pluviometer was installed at 2588 m in the Collarada Massif, to measure the amount of precipitation and temperature at higher elevation in the catchment. The theoretical amount of rainfall infiltration, is calculated as water excess by subtracting the potential evapotranspiration (Thornwaite, 1954) from the monthly precipitation sum.

3.3. Cave air monitoring

Cave air monitoring includes temperature, relative humidity (RH) and CO_2 air concentration (Fig. 1c). Temperature and RH were recorded hourly by four HOBO U23-001 temperature sensors (red circles in Fig. 1c). Temperature was also recorded by pressure sensors that measured air and water temperature (P_A and P_W in Fig. 1c, respectively). The CO_2 concentration was measured in the Cathedral room at 1-h interval (with sampling interval of 4 min) since January 2019, using a CO_2 transmitter HD37VBTV.1 (GHM Group) coupled to a U30-NRC HOBO station. In addition, monthly CO_2 measurements were taken from September 2018 to January 2021 at 9 sites in the cave and outside the cave entrance (green circles in Fig. 1c) using a handheld CO_2 instrument AZ-001. Cave air was sampled for $\delta^{13}C$ isotopes at the same sites, from January 2020 to January 2021, using 5.9 ml glass bottles with septum caps (Labco Exetainer). Each vial was opened at the sampling site and drained with a 60 ml syringe, allowing cave air to enter the vial, which was then sealed with a double wadded cap. A total of 122 air samples were analysed for CO_2 concentration and $\delta^{13}C$-CO_2 (VPDB) using a Picarro G2101-i analyser with cavity ring-down spectroscopy (CRDS-WS) (Crosson, 2008).

3.4. Hydrological monitoring

At the Cathedral room, a drip was monitored at weekly intervals (D-0 in Fig. 1c), between July 2017 and June 2021, with manual measurement of the drip rate (drops/second) and measurement of the amount of water collected under the drip (ml/week). Water pressure sensors were installed in November 2017. Water level was recorded every 15 min by using HOBO U20L-02. Water level was calculated after correcting for the atmospheric pressure using a sensor located at the sinkhole (purple circle in Fig. 1c). These sensors also recorded temperature variations every 15 min. The alarm system installed in the ramp connecting the phreatic and the tourist level, comprises 3 buoys at 4.70 m (lower level), 8.20 m (middle level) and at 14.50 m (higher level) from the pressure sensor (Pw in Fig. 2). An SMS with the exact time is automatically sent when the water reaches (or drops below) each buoy level (resolution up to the minute). All the warning messages sent since 2015 were recovered. Water flow was calculated from salt measurements at different water levels. A total of 16 salinity measurements were made during 8 hydrological events that flooded the tourist gallery. Piezometric changes in the karst water table were evaluated in a borehole 270 m from the cave, at an elevation of 958 m a.s.l. The timing of the hydrological response of each flood event was characterized using the water level data recorded in the cave, the rainfall data from the Canfranc gauging station and the snow height data from the Izas snow gauge station. The time lag was calculated for each flood event, as the difference in time between the centre of gravity of the hyetogram (for rainfall or snow melt rate) and the peak flow, given by the maximum water level in the hydrograph.

4. Monitoring results

4.1. Cave atmosphere

4.1.1. Ventilation regime, air temperature and relative humidity

Air currents are easily perceptible in the cave where gallery narrows, such as at the main entrance, the passage to the Cathedral, and the stairs connecting the tourist zone with the upper galleries (Fig. 1c). In the innermost part of the upper gallery the air flow is imperceptible. Our field observations indicate a bidirectional air flow at the four entrances, which is more pronounced at the main entrance with an inward airflow speed of up to 1.6 m/s and an outward airflow speed of up to 2.4 m/s. The presence of four entrances, with a maximum height difference of 42 m between the lower and the upper entrances, creates a chimney effect. When the outside temperature drops below that of the cave, the warm cave air rises towards the upper entrance, generating an upward airflow. Mass conservation implies that cold air is drown in at the lower entrances, effectively cooling the lower galleries. When the outside air is warmer than the air inside the cave, a reverse air flow occurs. Buoyancy forces drain the cold and denser cave air to the lower entrance and hot air enters through the upper entrances, thus describing a downward airflow ventilation regime. Downward airflow takes place mostly in summer although it occurs throughout the all year. Upward airflow is observed on cold winter days. Winter days with high thermal oscillation show outward ventilation at central hours and inward ventilation at night. Otherwise, the occurrence of external wind in the cave has been observed, generating more intense and gusty air currents.

Seasonal temperature variations are observed throughout the cave, with higher values in summer and lower values in winter. Cave air temperature showed large thermal oscillations up to 13.8 °C for sensors T-1, T-2 and T-3, located in a well-ventilated area, with a mean temperature of 8.2 °C, 8.9 °C, and 10.2 °C respectively (Table 1). These sensors are highly influenced by external temperature variations. Sensor T-1, located near to the lower (main) entrance, records a higher variability in winter, while sensor T-3, located in the upper gallery, correlates better with the external summer temperature (Fig. 2). Sensor T-2, located in an intermediate position, has the widest range, with values similar to T-3 in summer and values similar to T-1 in winter (Fig. 2). Sensor T4, located in the innermost part of the cave shows low thermal oscillations, (amplitude of 0.6 °C and a mean temperature of 10.8 °C). From the main entrance to the inner part of the cave, the temperature gradually increases from 8.2 °C to 10.9 °C (Table 2). During winter,

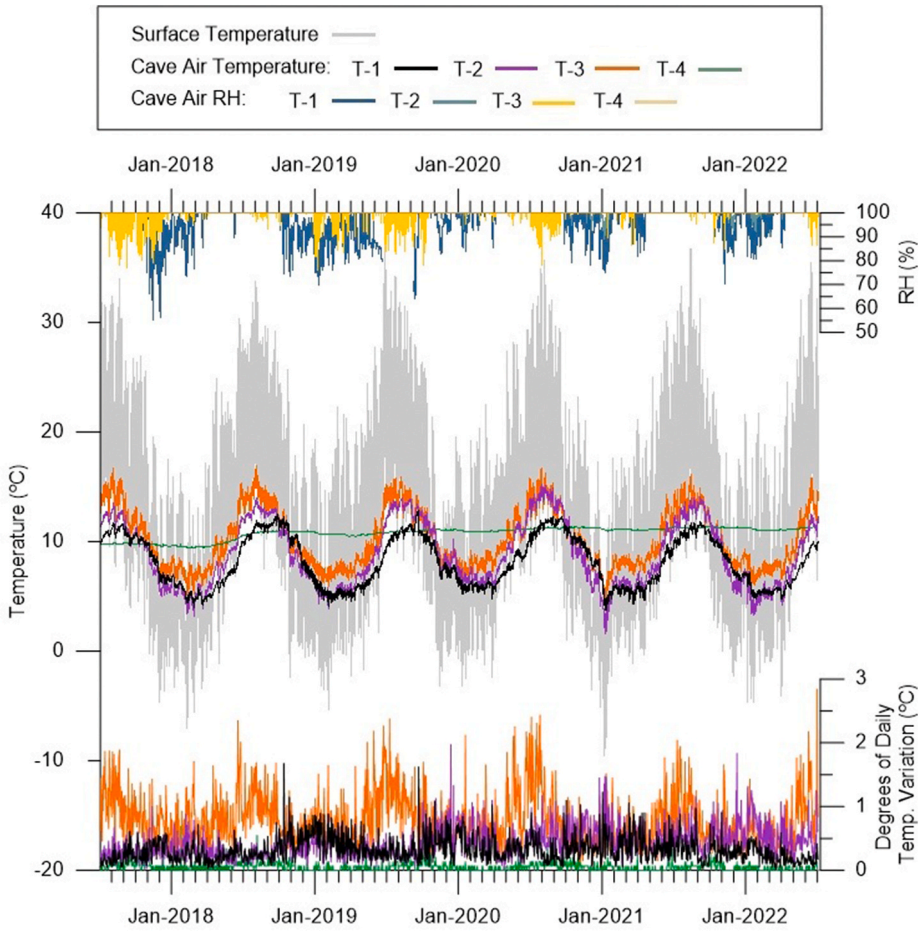

Fig. 2. Hourly records of air temperature and RH along the cave measured in sensors T-1, T-2, T-3 and T-4. The record of the outside temperature is shown with a grey line. Degrees of daily temperature variation is shown in the right-down axis for sensors T-1 to T-4.

Table 1
Summary of the mean, maximum and minimum values of air temperatures recorded in the LGSC and outside during the five years of the monitoring survey (from July 2017 to June 2022). Daily variation of temperature data for the same sensors and period is also indicated. These values are not shown for temperature of sensors P_A and P_W due to several interruptions in their recording, which makes it not possible to generate statistical values for the entire monitoring period. Temperature values of the outside air correspond with data recorded in Canfranc meteorological station.

	Temperature (°C)					Daily variation of Temperature (°C)		
Sensor position	Mean	Maximum	Maximum date	Minimum	Minimum date	Mean	Maximum	Minimum
T-1	8.2	12.8	September 22, 2019 16:00	3.7	January 08, 2021 08:00	0.33	1.68	0.03
T-2	8.9	15.3	August 01, 2020 21:00	1.5	January 08, 2021 10:00	0.43	1.97	0.03
T-3	10. 2	16.9	August 05, 2018 22:00	4.3	January 08, 2021 10:00	0.80	2.85	0.05
T-4	10.8	11.4	October 04, 2021 07:00	9.4	February 27, 2018 14:30	0.02	0.25	0
Outside	11.1	37.1	June 28, 2019 16:00	−9.6	January 06, 2021 08:15	10.8	21.8	1.5s

Table 2
Mean Annual Temperature (MAT) for sensors T1 to T4 in the cave and outside.

Year	MAT (°C)				
	T-1	T-2	T-3	T-4	Outside
2018	8.2	8.7	10.2	10.3	10.6
2019	7.9	9.0	10.0	10.8	11.1
2020	8.7	9.5	10.4	11.1	11.2
2021	8.0	8.7	10.1	11.2	10.7
2022	8,6	9.2	10.8	11.3	12.4
Average 2018–2022	8.3	9.0	10.3	10.9	11.2

icicles form between the main entrance and the Cathedral indicating that the temperature occasionally drops below 0 °C, as recorded at sensor P_A located at the sinkhole (minimum of −7,01 °C on January 6, 2021). The maximum temperatures were recorded between June and October (Table 1). In summer the highest temperature values are reached in the fossil galleries, near the upper entrances E3 and E4, as is shown at sensor T-3. The minimum temperature was reached during the Filomena Storm that took place between the 6th and January 10, 2021, except for sensor T-4 where minimum values were recorded in February 2018 (Table 1). Small daily variations in the cave air temperature are shown at T-1, T-2 and T-3 (Table 1). At sensors T-1 and T-2 the daily variations are slightly higher in winter. Daily temperature variations at sensor T-3 are higher in summer, corresponding to the largest daily variations measured in the cave (Fig. 2). In contrast, the daily variations at sensor T-4 are barely noticeable, although variations of around 0.1 °C are shown in autumn. In detail, daily outside temperature variations are reflected at T-1, T-2 and T-3 with a small delay of 1–3 h in winter and a larger delay of 5–10 h in summer. An increase in the annual mean

temperature of 1° is recorded for sensor T-4 during the monitoring period (Table 2).

T-1 and T-2 show important drops in RH during autumn and winter. In the upper gallery, T-3 shows drops in RH mainly during summer, while in T-4 the RH remains constant and close to 100%. In the records of sensors T-1 and T-2, drops in the RH of the air are observed when the outside temperature decreases below the temperature inside the cave (Fig. 2), which is easily noticeable during sudden temperature drops.

4.1.2. Monthly CO_2 concentration and $\delta^{13}C$-CO_2 air cave data

The monthly CO_2 concentrations measured manually at 10 sites along the cave (Fig. 1c) show important spatial differences. CO_2 values at control points A-2 to A-4, located in the tourist zone, remain low during the whole year (mean 425 ppm), while there is an increasing trend in CO_2 values towards the upper galleries (Fig. 3). The CO_2 concentration at A-5 and A-6, located at the beginning of the upper galleries, is slightly higher than the values of the tourist zone (mean about 450 ppm). Finally, the CO_2 concentrations at control points A-7 to A-10, located in the innermost part of the upper gallery, show higher values and great variability along the year (Fig. 3). A well reproduced seasonal pattern is observed in the CO_2 concentration data at all control points although it is barely perceptible in the tourist area (Fig. 3). In winter, CO_2 values remain low and homogenous throughout the cave (i.e. 416 ± 65 ppm). On the contrary, there is a general increase in CO_2 concentration during summer-autumn, particularly marked in the upper gallery. Summer CO_2 values show an increasing trend from control point A-7 towards the end of the gallery, reaching values up to ~7600 ppm at A-10. While the higher CO_2 values are only measured in the poorly ventilated areas of the cave, CO_2 levels decrease throughout the cave in autumn, together with decreasing external temperature.

The $\delta^{13}C$-CO_2 values in the cave air samples show similar spatio-temporal variations than the CO_2 concentration, with depleted $\delta^{13}C$ values when the CO_2 concentration is high, as shown by the correlation in the Keeling model (Fig. 3b). The $\delta^{13}C$ mean is −12.1 ‰ (±2.9 ‰), while the minimum (−21.4‰) and maximum (−9.3‰) are measured in August (A-10) and January (A-4), respectively. The most depleted $\delta^{13}C$ values are measured the innermost part of the cave during the summer, while the most enriched $\delta^{13}C$-CO_2 values are measured in the tourist zone in winter (Fig. 3). The largest contrast in the $\delta^{13}C$-CO_2 values between the upper galleries and the middle galleries is observed in summer, with a difference of 10.8‰ in September 2020.

4.1.3. Hourly CO_2 concentration data

The hourly CO_2-record in the Cathedral room (Fig. 1c) allows a

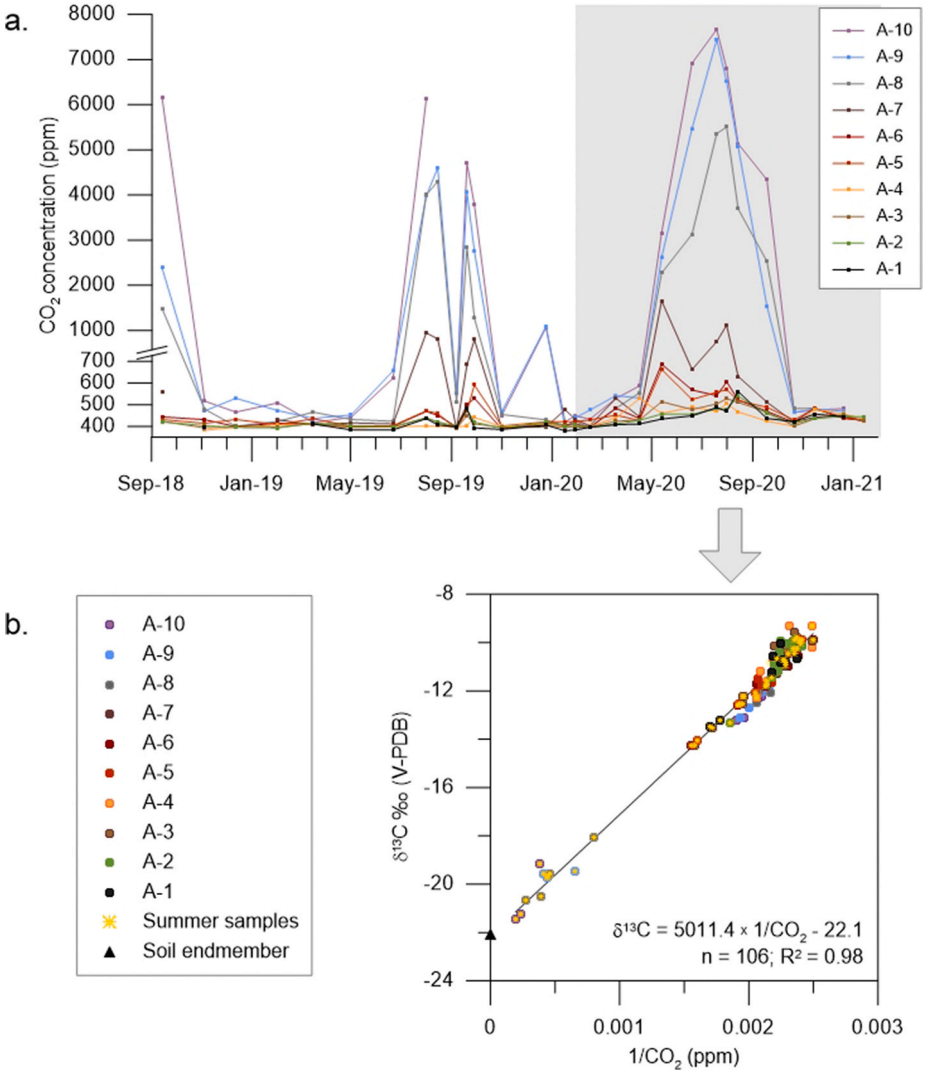

Fig. 3. **(a)** Monthly CO_2 concentration variation measured at the control points along the cave (A-2 to A-10) and outside (A-1). **(b)** Keeling plot ($\delta^{13}C$ vs $1/CO_2$) over data of air samples analysis showing positive and high correlation coefficient ($R^2 = 0.98$), with higher CO_2 concentrations corresponding with isotopically depleted carbon and occurring during summer.

detailed analysis of the temporal CO_2 variation. The mean CO_2 concentration at this station was 427 ± 35 ppm with a daily variation of about 25 ppm, with higher values at night and lower values at noon (Fig. 4a). This daily variation is clearly observed during days without visits (e.g. during the lockdown), in the absence of anthropogenic CO_2 contributions. The anthropogenic signal occurs during the daytime, when natural CO_2 levels are lowest, blurring the natural CO_2 variation (Fig. 4a).

Groups of between 20 and 35 people visit the cave for 1 h in a usual regimen of two visits per day that take place at 12 noon and 6 p.m., increasing to four visits per day at weekends depending on demand. The visitors' breathing quickly increases the cave pCO_2 by ~100 ppm (Fig. 4c d) depending on the number of people, although these parameters are not always correlated. These peaks are generally reduced when the visitors leave the cave and the cave air pCO_2 returns to the background level within 30 min to 2 h. Exceptionally, during high tourist seasons (e.g. Christmas, Easter and summer holidays), the number of visits increases up to 6–8 visits per day for several consecutive days, resulting in a longer recovery time with levels returning to atmospheric conditions overnight (Fig. 4b). There is no clear correlation between the recovery time and the number of visitors, suggesting that CO_2 fluxes depend mainly on the ventilation rate, which is variable over time.

On an interannual scale, there is an apparent positive correlation between the number of visits and the variability of CO_2 in summer and winter (Fig. 4c), with high CO_2 levels in August, when the highest

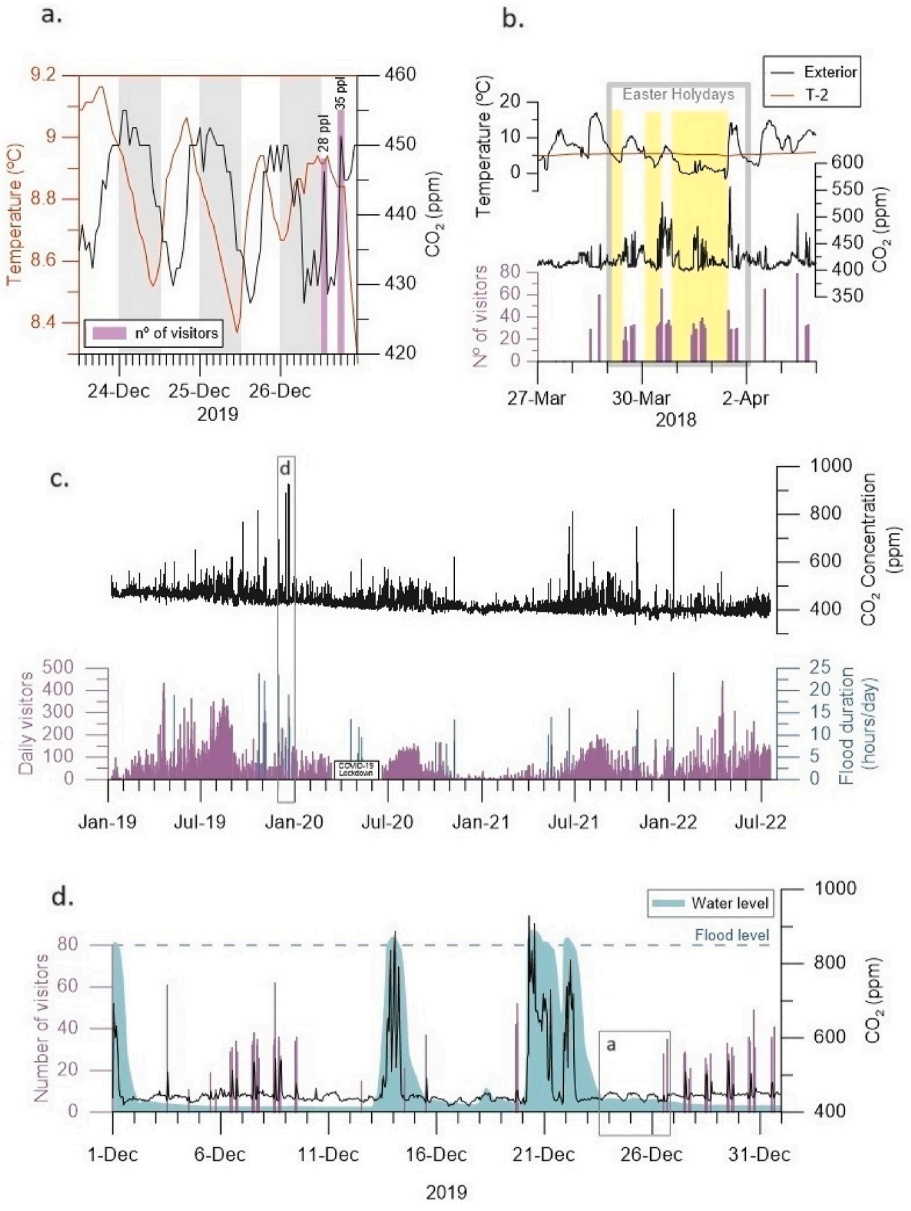

Fig. 4. **(a)** Detail-window shows daily variation of CO_2 (black line) and temperature (red line) at the Cathedral room during three consecutive days without visits. About 25 ppm daily variation is clearly shown with maximum values at the middle of the night and minimum values at the beginning of the evening. CO_2 increases due to visitors' breathing are shown on 26th December. **(b)** CO_2 concentration and number of visitors during Easter holidays 2018. The increase of visitors produces increases in CO_2 that are maintained several hours without recovering the background values. Yellow shaded areas indicate upward airflow ventilation regime when external temperature descends over the cave temperature. **(c)** Hourly record of CO_2 concentration measured at the Cathedral room, number of visitors in the cave per day and number of hours of flood in the tourist gallery of LGSC. **(d)** Variation of the CO_2 concentration (black line) and water level (blue filled line) compared with the number of visitors in the cave during several days in December 2019. The dashed line indicates the level of water that causes flooding of the tourist part of the cave. (For interpretation of the references to colour in this figure legend, the reader is referred to the Web version of this article.)

number of visitors occurs, and low CO_2 levels coinciding with the lower number of visitors in winter (e.g. winter 2021). However, this effect is not clearly evident during the 3-month period without visits due to the lockdown derived from the COVID-19 pandemic restrictions (Fig. 4c). Furthermore, a detailed analysis of the CO_2 variation during a period of high affluence of visitor allows to identify lower recovery rates during the upward ventilation mode, when the external temperature drops over the cave temperature (Fig. 4b). As the visit is a round trip (entry and exit through entrance E1), visitors pass by the Cathedral CO_2 sensor twice. Thus, with upward ventilation, the anthropic CO_2 is effectively eliminated from the Cathedral room. Conversely, with downward airflow, the CO_2 from visitors while they visit the rest of the cave, is led towards the Cathedral area, where a higher rate of CO_2 can be observed throughout the visits time.

Large CO_2 peaks observed in this record are not correlated with visits, but correspond in time to flooding in the tourist area. These sudden CO_2 increases are caused by the degassing of water during the floods and correspond to the highest peaks in the CO_2 concentration record, with a maximum value of 929 ppm (Fig. 4d). The CO_2 values drop drastically as the water descends towards the siphon (Fig. 4d), affecting the cave atmosphere only during the flood duration. Anthropogenic CO_2 emissions are much lower than those induced by flooding, and both are rapidly removed by the strong ventilation regime.

4.2. Cave hydrology

4.2.1. Cave water response to precipitation

Hydrological recharge is maximum between autumn and winter (Fig. 5a). In the high part of the massif (above 2000 m a.s.l.), infiltration in winter and spring is the sum of water excess and snow depth (Fig. 5a b.). In summer, water excess values are negative. The drip rate control point at the Cathedral room shows high values of discharge and high variability throughout the year (Fig. 5c), recording a maximum discharge of 806.4 ml/day. At the beginning of summer, this seepage shows discharges around 200–400 ml/day that decrease towards the end of summer when it dries out completely. This seasonal variation is directly related to the water excess (Fig. 5a c).

The record of the water level in the LGSC shows steady values that increase during short events of variable duration (a few hours to several days), correlating with high infiltration periods (Fig. 5a e). In spring, when the phreatic level is high, a rise in the water level can be caused by snowmelt. When the water rises ~15 m from the pressure sensor (P_W in Fig. 2), it reaches the higher buoy and a flood alarm is triggered (red dots in Fig. 5e). Water exceeding this level (980 m a.s.l.) overflows through the tourist gallery. A total of 52 floods events occurred in the tourist gallery during the monitoring period. 34 floods occurred in spring (62%), 16 in autumn (29%), 4 in winter (7%) and one in summer (2%). The number of annual floods and their duration have decreased over the monitoring period (Fig. 5e). This decreasing trend is confirmed by the alarm messages recovered since 2015. The temperature of the phreatic water measured in the siphon varies along the year, with the lowest

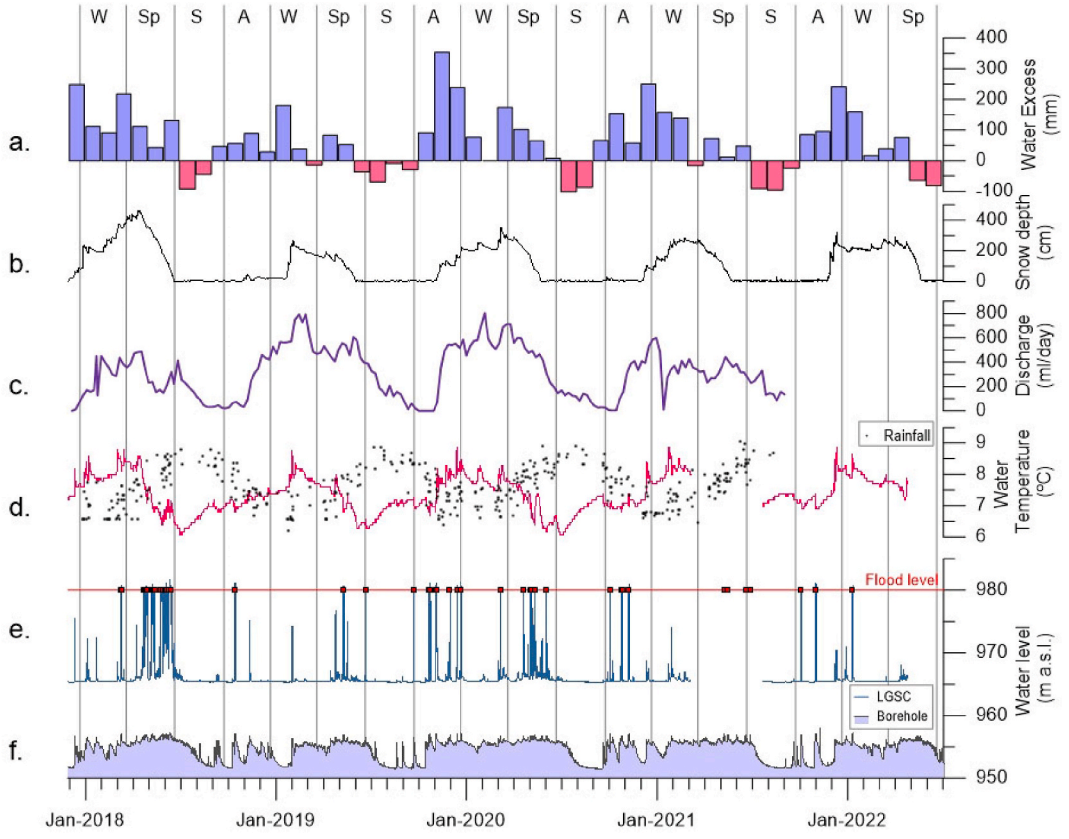

Fig. 5. **(a)** Water excess calculated as monthly amount of precipitation minus evapotranspiration and representing the amount of rainfall that infiltrates into the soil. **(b)** Snow depth at Izas station (2086 m a.s.l.). **(c)** Drip rate variation of drip D-0 at the Cathedral room. **(d)** Water temperature in the LGSC siphon area and rainfall temperature measured at the Interpretation Centre rain gauge in Villanúa. Rainfall temperature data are not scale, showing only higher and lower temperatures than cave water. **(e)** Water level recorded at the siphon area of the cave. The red line indicates the water level from which the tourist gallery starts flooding (height of the maximum level flood alarm). The red dots indicate the record of the maximum level flood alarm. **(f)** Piezometric level measured at Villanúa borehole, for the monitoring period. The vertical bars separate the different seasons (W: winter, Sp: spring, S: summer, A: autumn). (For interpretation of the references to colour in this figure legend, the reader is referred to the Web version of this article.)

values in summer and the highest in winter (Fig. 5d), within a range of 2.8 °C (8.9 °C maximum; 6.1 °C minimum; 7.4 °C mean temperature). The water temperature is controlled by the precipitation temperature. Thus, there is a seasonal decrease in temperature that correlates with the spring snowmelt which causes the influx of cold water into the karst system (Fig. 5b d). From the end of spring to the beginning of the autumn, the rainfall temperature is higher than the phreatic water temperature and large amounts of rainfall increase the phreatic water temperature punctually, even during the cooling caused by the snowmelt infiltration (e.g. temperature increase in May 2018, Fig. 5d). On the contrary, meteoric precipitation during autumn, winter and part of spring, has lower temperature than the phreatic water and leads to a decrease in cave water temperature (Fig. 5d). At the beginning of winter, the increase in groundwater temperature continues despite cold precipitation events (Fig. 5), as large amounts of snow accumulate on the surface without generating infiltration. The piezometric level at the CHE borehole shows clear seasonal variations in the range of 6 m (Fig. 5f). Low water levels (~952 m a.s.l.) occur during summer. In autumn, the piezometric level rises, while the longest period of karst water storage corresponds to winter and spring (~956 m a.s.l.). The record of the piezometric level shows a decreasing trend in the water head since 2009 until today (Fig. S1; supplementary). Comparing the records of the piezometric level and the cave water level, a height of 956.75 m a.s.l. (−1.25m from the surface) is observed in the borehole when the water floods the tourist gallery of LGSC, that is when the water reaches the level of 980 m a.s.l. in the cave. This reference level led us to compare the variation in the number of flood events in the LGSC since 2009 (Fig. S1), and to observe a decrease in their frequency. On the other hand, the flow rates measured at the spring of LGSC during the summer draught range approximately between 10 and 100 l/s.

4.2.2. *Identification and characteristics of floods in the cave*

Table S2 lists 55 flood events during the monitoring period, characterized by duration, rate of water rise along the ramp from the siphon, maximum height reached by the water in the cave (peak flow), the estimated maximum flow rate in the tourist gallery, and the response time to the associated meteoric precipitation. The duration of the flooding in the tourist gallery is highly variable, ranging from less than 2 h for event 26, caused by rain, up to 55 h for event 21, caused by snowmelt. The water rise through the siphon ramp is also highly variable, ranging from 1 to 29 cm/min. Low rates of rise are generally associated with the snowmelt while fast rises of the water level are usually related to high-intensity rainfall events. The fastest rises occur in autumn, when water level rises up to 29 cm/min were observed (October 2018). The flow rates measured in the tourist gallery range from 28 l/s at the beginning or at the end of the flood to 985 l/s close to the peak flood. The flow rates are linearly correlated with the water level measured at the siphon ($R^2 = 0.98$): Q = 848.87*H-12435; where Q is the flow rate in the tourist gallery in l/s and H is the height of the water level in the cave in m. This allows the estimation of the maximum flow rate reached during the flood (Table S2).

The time lag for floods is also very variable; some examples of flood events are shown in Fig. 6, together with the corresponding rainfall/snowmelt event. For those floods that are caused by rainfall events, the response time depends on the duration and intensity of each precipitation event. Therefore, we have analysed the water level rises caused by precipitation with a uniform spatial distribution on the massif and in the valley, where 15-min precipitation data are available. Short and isolated rainfall events have a time lag of 8 ± 1 h (e.g. event 43 in Fig. 6). For long rainfall events, even several days, the time lag is not easy to calculate because it is difficult to define the rainfall event causing the flooding situation (e.g. the rainfall at the beginning of event 29 in Fig. 6). In these cases, time lags of more than 10 h are expected. Once the

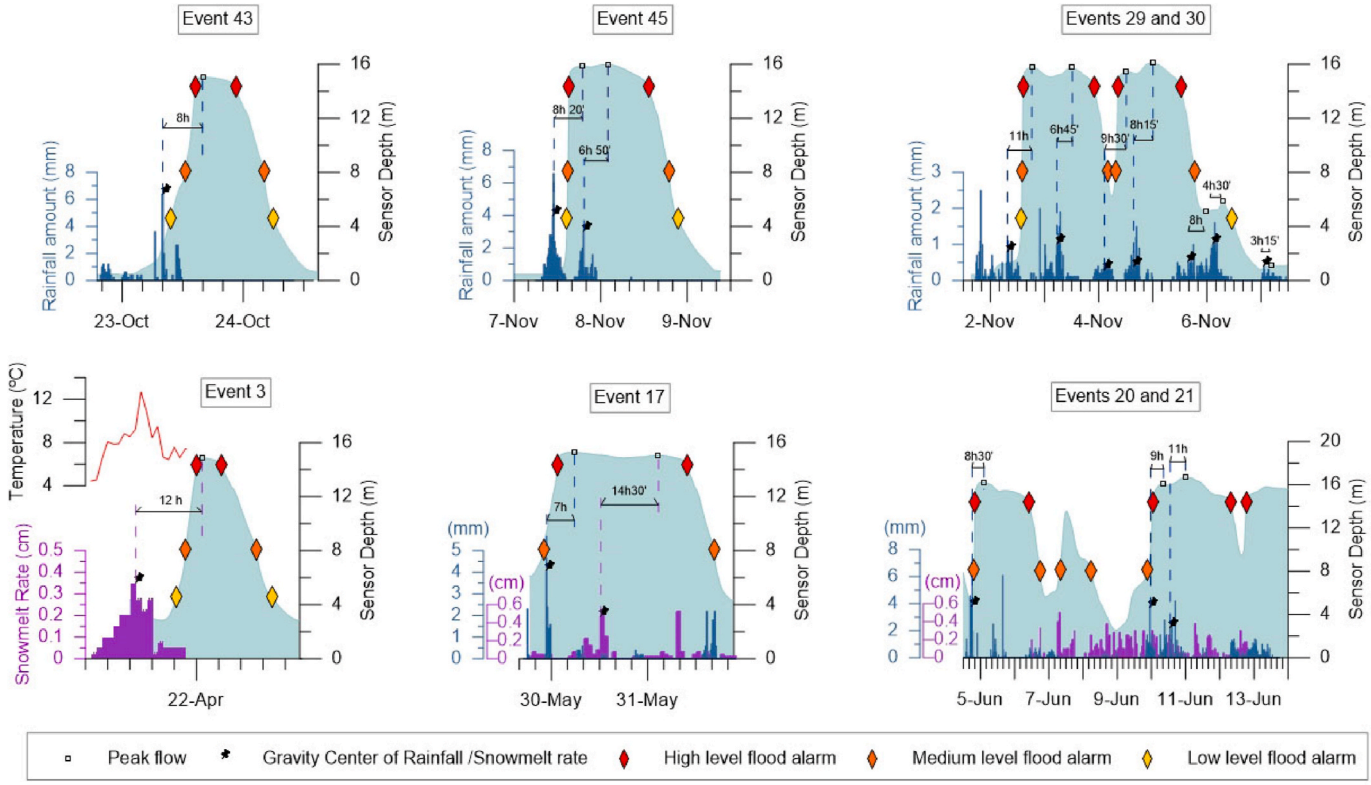

Fig. 6. Hydrographs of some cave flooding during the monitoring period. 15-minutes rainfall amount data (blue bars) or 15-min snowmelt rate data (purple bars) are indicated. Note that they are represented with different scales for each event. See also Table S2 for the detailed characterization of every flood event. (For interpretation of the references to colour in this figure legend, the reader is referred to the Web version of this article.)

water level is high and the cave is flooded, the time lags for subsequent rainfall are much shorter (e.g. events 45, 29 and 30 at Fig. 6). In the case of floods caused by snowmelt only, the time lags are longer and quite stable (12.5 ± 1 h) and depend on the outside air temperature (e.g. event 3 in Fig. 6). These time lags were calculated using the snowmelt recorded at the Izas station, as input to the karst system. When snowmelt and rainfall are mixed, a more detailed analysis is required to obtain time lags. Sometimes, several peaks are observed during the same flood event (e.g. event 17 in Fig. 6) and time lags are more variable and usually longer (e.g. events 20 and 21 in Fig. 6).

The amount of rainfall required to produce a flood is variable, with low values when the phreatic level is high, such as during the snowmelt (e.g. mixed precipitation regime events 8, 13, 15, 46, Table S1). For events caused only by rainfall, the highest frequency of flooding occurs for rainfall greater than ~20 mm. This rainfall amount may be lower for long rainfall-flood events.

The characteristics of the flood response related to hydrological recharge are illustrated in two general situations described in the supplementary material. In the first situation (Fig. S3), during the spring season of 2018, snowmelt and rainfall increase, while in the second situation, occurring in summer of 2019 (Fig. S4), there is a hydric deficit and rainfall shows a stormy behaviour. In summer, some increases in the cave water level do not correlate with precipitation data in either Canfranc or Villanúa, showing a correlation with rainfall in the Collarada high altitude zone (Fig. S5), where the main recharge of the karst system takes place. This situation shows the effect of rainfall distribution at different altitudes and illustrates the discrepancy between the local rainfall record at the cave site and the effective recharge observed in the hydrological catchment of the cave.

5. Discussion

5.1. Cave dynamics and CO_2 sources

The cave is well ventilated as a consequence of the air currents taking place between the upper and lower entrances. Temperature differences between the external and internal air control the air density differences that induce a chimney effect and determine air renewal. Sensors T-1, T-2 and T-3 record high thermal oscillations suggesting that temperature changes are mainly controlled by advection as a consequence of ventilation processes. On the contrary, sensor T-4 in the innermost zone of the cave shows a relative thermal stability, indicating limited heat exchanges due to limited circulation in absence of a direct connection with the outside. Daily temperature variations at T-3, which are pronounced in summer, suggest that T-3 is more influenced by entrance E4 throughout the year under the downward ventilation regime that dominates in summer. Temperature at sensors T-1 and T-2 is most influenced by external temperature in winter, under upward ventilation regime (Fig. 2). However, since T-2 is more dependent on the external temperature in summer than T-1, and the daily temperature variation in winter is higher at T-2 than at T-1, we assume that temperature at T-2 is more influenced by airflows taking place through the entrance E3, under downward ventilation, even in winter, when both downward and upward airflows alternate. Therefore, the annual mean daily amplitude is higher at T-2 than at T-1 because it is more influenced by E3 for most of the year. Thus, the external temperature controls the ventilation regime in the cave. Otherwise, external daily temperature oscillations are reflected inside the cave with a smaller delay in winter (1–3 h) compared to summer (5–10 h), indicating an effective cooling during upward ventilation. Relative humidity (RH) drops recorded at T-1 and T-2 during autumn and winter are related to the entrance of cold and dry air into the cave, associated with the main entrance and the E2 entrance. The low RH recorded at T-3 in summer is probably due to the entry of warm external air through the upper entrances (E3 and E4). T-1 shows temperature values below the external mean for the most of the year (Fig. 2), due to the asymmetric air flow associated with the chimney effect, which creates a negative thermal anomaly at the lower entrance. Otherwise, T-1, T-2 and T-3 records show differences in annual variation, with closer values during the autumn cooling period and more different values during the rest of the year (Fig. 2). The effective cooling of the upper galleries in autumn may be enhanced by thermal convection, which facilitates the entry of cold, dense air through the descent passages from the lower entrances, by creating gravity flows. Cold air can also enter through the descent passage from entrance E3, facilitating the rapid cooling observed at sensor T-3 (Fig. 2).

The strong ventilation creates a continuous exchange of air with the outside, preventing the accumulation of CO_2 in the tourist zone, as shown by the monthly data from A-2 to A-6 control points, with values similar to the external atmosphere. On the contrary, there is a trend to higher CO_2 concentration towards the inmost zone of the cave, where there is no connection with the outside air atmosphere, barely noticeable in winter but much clearer in summer. The accumulation of warmer air in the highest galleries of the cave prevents ventilation in summer, when the outside temperatures are very high. When the outside temperature drops below the cave air temperature and induces an upward airflow, the upper galleries connect to the external atmosphere, allowing the removal of CO_2 (e.g. decrease in CO_2 levels at A-5 and A-6 control points in June 2020; Fig. 3a). A larger drop in temperature allows air renewal even in areas without connection to the outside (e.g. decrease in CO_2 levels at stations A-8, A-9 and A-10 in September 2019 and September and October 2020; Fig. 3a). Theses air renewal events coincide with very small daily variations at T-4.

The ventilation dynamics described for LGSC corresponds to that defined by Faimon et al., (2012) for a two-entrance dynamic cave in the Moravian Karst, where three ventilation modes were distinguished: upward airflow, downward airflow and transitional mode when a switching between upward and downward airflow occurs. The results of this study identified the air circulation as changing the pattern of temperature distribution according to the ventilation mode and ventilation period, similar to what happens in LGSC. It also quantified the highest airflows under extreme external temperature conditions. The transitional mode was characterized by a stagnant ventilation period occurring when the annual external and cave temperatures are similar (Faimon et al., 2012). The four entrances in the LGSC induce different airflow directions in the different sections of the cave during the transitional mode, resulting in a gradual change. The influence of outside wind on cave airflows has also been reported in other caves (Mattey et al., 2021). A continuous recording of the air flow at the four entrance passages of the LGSC would allow the dynamics of this transitional mode to be precisely defined as well as the wind incidence on the ventilation dynamics.

CO_2 sources in the tourist gallery, associated with visitor's breathing and water degassing during flooding were inferred from the hourly CO_2, water level and number of visits records. However, these relationships do not exist for the non-ventilated galleries where the greatest variation in annual CO_2 concentration occurs. The $\delta^{13}C$ measured in CO_2 has been used as a geochemical tool to identify the source of CO_2 in caves (Gázquez et al., 2016; Mandić et al., 2013; Spötl et al., 2005). The $\delta^{13}C$-CO_2 values measured in winter (January 2021), similar to those of the outside atmosphere, support the ventilation and homogenization processes explained above. In summer, $\delta^{13}C$-CO_2 values are more negative at stations A-2 to A-6 (mean of −12.5‰ in August 2020), similar to the external atmosphere, and more depleted values in the innermost A-8 to A-10 control points (up to −21.4‰). These values are similar to the edaphic $\delta^{13}C$-CO_2 values on a global scale, which range between −26‰ and −12.5‰, being more depleted when CO_2 is derived from C_3-type plants respiration (Breecker et al., 2012; Mattey et al., 2021; O'Leary, 1981). The two-endmember Keeling plot (Fig. 3b) gives a value of −22.1‰ in the cut with Y-axis, representing the $\delta^{13}C$-CO_2 value of the soil end-member. Thus, since the boxwood forest developed in the soil overlying the LGSC, it is expected that depleted $\delta^{13}C$ values were supplied by edaphic CO_2 when drip water degassing occurred in the

cave. Many studies propose drip water degassing as a process that produces an important CO_2 contribution into caves (Li et al., 2024; Mandić et al., 2013; Mattey et al., 2016, 2021). The depleted $\delta^{13}C$ values shown in the innermost areas during summer are consistent with a spring seepage recharge, which may input CO_2 that gradually degasses in this area, where there is no ventilation. Similar results have been found in other shallow caves (Li et al., 2024) where seasonal signal in cave air $\delta^{13}C$ and CO_2 concentration results from the interplay between soil dynamics and cold-season ventilation. In addition, the presence of bats in the upper galleries throughout the year may introduce alternative biogenic CO_2 sources (Holcomb, 2016). Otherwise, the contribution of CO_2 water degassing from the active stream at the lower level, through the narrow eastern connection (Fig. 1c), should not be ruled out. A more comprehensive analysis of $\delta^{13}C$ from these potential sources would be required to determine their effective contribution to the CO_2 flux.

The environmental monitoring of LGSC contributes to our knowledge of the cave ventilation which is controlled by external temperature and affects mean cave temperatures, cave CO_2 fluxes, and thus, the drip water geochemistry (Mattey et al., 2021). Consequently, this study also provides knowledge about the impact of climate on cave processes such as speleothem growth, which will be essential for future paleoclimatic studies based on speleothems.

5.2. Karst response to meteoric precipitation

The correlation between the drip rate variability and the infiltration in the karst system (Fig. 5a c) shows a rapid response of the seepage to precipitation. The decrease in drip water towards the end of the summer season is attributed to a lower water saturation of the epikarst, together with a high evapotranspiration that inhibits its recharge during rain events. In autumn, as the outside temperature decreases and rainfall becomes more effective, the epikarst recharges, thus increasing drip rates in the cave during autumn and winter. Snowfall produces a slow infiltration that is reflected in the cave with higher drip rates over several days. The water level rises sharply, indicating a rapid response to precipitation and reflecting a concentrated recharge associated with a well-developed cave system (Jakucs, 1959; Worthington, 1994). During floods, the time lag, the speed of water rise along the siphon ramp and the flood magnitude are highly variable and depend not only on the amount of water stored but also on the type of precipitation. The spatial distribution of the meteoric precipitation, the duration of the rainfall event and the intensity of the precipitation as well as its distribution during the event determine the response of the water level in the cave (Fig. 6). The response time of the water level to the precipitation event varies between 6 and 22 h, although most rises react within ~8 h. After several days of rain or snowmelt, with high water levels in the system, response times can be much shorter.

The amount of precipitation required to reach the flood stage and the frequency of floods vary throughout the year. Consequently, the water level in the cave rises more frequently in spring and in autumn (Fig. 5e) when the rainiest periods occur. In winter, rainfall is usually evenly distributed, with similar values at high altitudes and in the valley, but snowfall dominates at high altitudes, limiting groundwater recharge. Accordingly, the observed water levels remain low during this period and floods reach the tourist gallery only with occasional rainfall. However, towards the end of winter when rainfall increases, the water retained in the karst system increases and the water reaches the tourist area more easily, even with small amounts of precipitation. Generally higher water levels are observed in spring, when the water from snowmelt is added to the rainfall. Moreover, daily water level fluctuations are observed without precipitation events only in relation with snowmelt (Table S2 and Fig. S3), reaching their maximum at night. During the summer, a background level is maintained with little water retained in the system and, only events characterized by a high amount of precipitation are able to raise the cave water level sufficiently to flood the tourist gallery. In addition, convective rainfall events, which occur mainly in summer, determine an irregular distribution of rainfall, concentrating large amounts of rainwater in small areas challenging the monitoring of the effective hydrological recharge. Therefore, the spatial character of summer storms is a very important factor to consider when evaluating the response of the cave water levels to rainfall.

During floods, the water level measured in the siphon correlates linearly with the flow rates measured in the overflowing stream. An increase in the phreatic level results in an increase in the volume of water overflowing through the tourist gallery. The variations in the water level are very small compared to the flow variations in the intermediate gallery, allowing large volumes of water to be evacuated easily.

6. Application of the monitoring study to the management of LGSC

The management of show caves, supported by environmental monitoring, allows measures to be taken to minimize human impact on the cave and increase visitor safety. In addition, guided visits offer an added value to the tourist product and support cave preservation by raising awareness of the fragility of the underground environment and encouraging its conservation. Meanwhile, the guide controls the behaviour of people in the cave, avoiding sources of dirt, breakage of speleothems, erosion of paths and other actions with irreversible negative effects on the cave. The scientific knowledge gained from the monitoring should be incorporated into the information provided to visitors in order to improve the quality of their visit. Furthermore, in caves with risk of flooding, the guide is the most important person to manage the safety of the visitors in the event of flooding. The final effect of this type of management is to reduce economic losses and increase the overall benefits.

6.1. Visitors impact on the cave and their management

Visitors don't seem to impact the air temperature in the LGSC. There is no direct relationship between the number of people entering the cave and the increase in temperature. However, this cause-effect relationship is difficult to evaluate because the number of people entering the cave varies in phase with the natural temperature changes, both on a daily and seasonal basis. Visits to the cave take place between 11:00 a.m. and 7:00 p.m., when the outside temperatures are at their highest. Similarly, the highest temperatures also occur in summer, when the number of visits and visitors multiplies by four. On the other hand, there are no variations in RH due to visits. Thus, it is possible to rule out the effects of the present tourist activity on the temperature and RH of the cave air and a potential impact on the cave ecosystem. Visitors breathing increases the CO_2 concentration levels but without a strong impact on the cave, because the ventilation is the main factor controlling the environmental conditions inside the cave galleries. In this way, the CO_2 recovery time is primarily controlled by the ventilation rates. In this respect, a larger number of people per visit would have a similar effect, even a smaller effect under upward ventilation. On the other hand, opening the upper galleries to tourism, including the non-ventilated areas, could expose visitors to high gas concentrations in summer. Furthermore, the impact of tourism in these areas could have negative effects on the cave environment.

6.2. Flood risk management

Flooding poses the greatest challenge to the proper management of the visits, especially during the spring and autumn months. The flood warning system is activated when the water reaches certain critical levels and remains active until water drops below the alarm sensor level. Currently, when the lower warning is activated, visits are immediately cancelled to avoid any risk to people. The cave remains closed to the public while the alarm is active, even if the water level falls back

towards the siphon area. This exemplifies a responsible management of the cave with safety as a priority, which increases the confidence and security of the visitors. In the case of a sudden rise in the water level during a cave tour, the alarm system inside the cave warns of the level reached by flashing lights. The guides are trained to evacuate people outside the cave in about 3 min, using either the main entrance or one of the upper entrances, depending on their location.

The training of managers and guides in the hydrodynamics of the cave system is essential to anticipate flooding. The results of monitoring contribute to enhance the guide's education and to reduce the uncertainties of the flood prediction. This facilitates the organization of visits and special events in the cave, improves the booking service during periods of high water and keeps the cave open for visitors, in particular when the water level is lowering. Knowing the hydrological response time is an important tool to anticipate the closure of the cave and organize visiting times. The amount of precipitation necessary to produce a flood is variable, depending on the amount of water stored in the system. However, the monitoring of the phreatic levels together with live data of precipitation amounts, allow predicting a flood at least 7 h in advance when the rainfall exceeds ~20 mm. Still, if rainfall persists, the rain amount needed for flooding may be smaller and the response times shorter. Conversely, during snowmelt, any amount of rain has the potential to produce a flood, with variable time lags. In addition, night floods caused only by snowmelt are expected during the period of snowmelt when minimum temperatures in the high mountain are above 0 °C. On the other hand, the irregular distribution of precipitation complicates flood prediction when events are caused by rainfall in the high mountain area. Incorporating a remote monitoring of precipitation with rain gauges in the catchment would allow flood risks to be accurately identified during storms in this area.

6.3. Economic management

The flooding of the tourist zone forces the cancellation of visits, generating economic losses for the company managing the LGSC. Short-term flood forces to close the cave only for a short period of time (one or two days) and, consequently, visits can be rescheduled, in most cases with minimal cancellations. However, these short floods produce greater losses when they coincide with high-occupancy periods during the Spanish vacations, including seasonal holidays in spring and autumn. An example of this occurred at beginning of November 2021 (All Saints' Day), when several special cave visits (more expensive) were cancelled because the cave remained flooded for three days, causing major economic losses. Spring is the season when a large number of schoolchildren visit the cave every weekday, but it is also one of the seasons with a higher risk of flooding. The highest number of days with the cave closed occurred in the spring of 2018 (Fig. S3). The continuous temperature variations triggered and stopped snowmelt throughout the spring, and the high rainfall observed at the end of the season, contributed to extend high water levels and caused recurrent flooding along the season (Fig. S4). The water flowed through the cave for 34 days and flood alarms remained active for a total of 45 days. This situation forced to close the cave for almost the entire school season. The management actions carried out in this situation, focused on minimize economic losses, consisted in directing the visits to the interpretation centre with the resources available and supporting the visits with the explanations of the guides. The economic losses due to cancellations caused by floods ranged between 1% and 5% of the total annual income. Present knowledge based on the monitoring could reduce the duration of lockdown in spring, thus reducing economic losses (e.g. considering that floods caused only by snowmelt affect the cave during the night). When the cave is flooded, the visit could be replaced by a view of the torrent of water in the cave from the main entrance, adapting a barrage to the current fence to prevent people from passing but allow safe observation of the spectacle, even using entrance E3 to access the Cathedral zone. This activity can be used to spread awareness of flooding, integrating the knowledge gained from monitoring the cave.

Tourist activity remains exposed to the occurrence of great magnitude floods with a low recurrence (extraordinary events), such as the exceptional event of October 2012. Extreme precipitation events can produce damages to the cave facilities leading to large economic losses and even human risks, if a sudden water rise takes place during a visit. The economic losses due to such extraordinary event are significant (e.g. the material investments in LGSC after the extreme flood event in 2012 accounted for almost the 100% of that year's profits). Under the current global warming and the projected increase in extreme hydrological events in Europe (IPCC, 2021), the management of the cave is complex in terms of coping with the magnitude and intensity of future flood events. For example, while precipitation in the Pyrenees is predicted to decrease (López-Moreno et al., 2008), the number of flash-floods is expected to increase (Llasat, 2021). However, recent studies point to the importance of other variables, such as changes in the seasonality of rainfall and/or soil moisture prior to rainfall events (Tramblay et al., 2023), as important facts to consider when analysing the long-term evolution of flood hazards. A tendency towards fewer rainfall events in the Pyrenees is already observed through the analysis of meteorological stations (Pérez-Zanón et al., 2017), a trend also detected during the monitoring period in the LGSC. In such a situation, the losses caused by floods in the LGSC are reduced and almost disappear in 2022, coinciding with the low snow accumulation in the mountains (OPCC-CTP, 2018). Thus, the climate change would induce a new situation with, potentially, a decrease in the annual flood rate along the cave. Still, it is important to monitor rainfall and flooding in the LGSC to determine whether minimal changes in other factors (e.g. rainfall seasonality, increase of extreme events) may lead to an increase in the occurrence of extreme flooding in LGSC in the coming years. In addition, future studies focusing on the hydrology, including hydraulic models (e.g. Bartolomé et al., 2024; Jeannin, 2001; Vuilleumier et al., 2019), will help to understand the dynamics of flooding. Thus, future research will help to anticipate flood hazards and risk management actions during the rainfall season, improving the safety of the visitors and additionally, avoiding economic losses as much as possible.

7. Conclusion

The monitoring of the Las Güixas show cave provides insights into the environmental and hydrological dynamics, which is useful for cave management. The main results of this work are related to the natural regulation of environmental processes in the tourist area, pointing to the strong ventilation due to the cave morphology and entrances at four different elevations as the main factor controlling the cave dynamics. The high thermal oscillation (up to 13.8 °C) measured in most parts of the cave is controlled by outside temperature variation through air advection. A non-ventilated area of the cave shows stable hygrothermal characteristics and higher summer values of CO_2 concentration. In the tourist zone, increases in the CO_2 concentration up to ~929 ppm are caused by water degassing during floods and inputs around 100 ppm are due to visitors. Both are rapidly removed due to the strong ventilation regime, recovering background values of ~425 ppm in 1 h approximately. The response of the seepage and the increase of water level inside the cave are both related to the amount of water recharged and stored in the karst system, which varies seasonally. The snow cover evolution in the catchment controls the aquifer budget and cave floods. The analysis of hydrographs during the flooding of the cave indicates a response time of about 8–12 h to the rainfall/snowmelt event. When the water stored in the karst system is high, mainly in spring, small rainfall (less than 20 mm) may trigger a rapid flood of the cave with a short time lag (less than 8 h). The irregular distribution of rainfall, which occurs mainly in summer, must be considered to forecast cave floods. Hydrological measurements are crucial for understanding flooding dynamics and assessing flood risks in tourist caves, particularly in epiphreatic zones. Ordinary floods have decreased in the current context of climate

change, due to reduced precipitation and changes in precipitation modes. However, extreme floods pose significant economic risks and their occurrence is a concern for the future.

Funding

This work was supported by an economic grant provided by the Ayuntamiento de Villanúa, the PYCACHU project (PID2019-106050RB-I00) funded by the Spanish Government and the MODKARST project (No. 101107943) funded by the European Commision.

CRediT authorship contribution statement

Reyes Giménez: Writing – original draft, Investigation, Funding acquisition, Formal analysis, Data curation, Conceptualization. **Ana Moreno:** Writing – review & editing, Supervision, Funding acquisition, Conceptualization. **Marc Luetscher:** Writing – review & editing, Conceptualization. **Lope Ezquerro:** Writing – review & editing, Investigation. **Antonio Delgado-Huertas:** Resources. **Gerardo Benito:** Writing – review & editing. **Miguel Bartolomé:** Writing – review & editing, Supervision, Methodology, Investigation, Funding acquisition, Conceptualization.

Declaration of competing interest

The authors declare that they have no known competing financial interests or personal relationships that could have appeared to influence the work reported in this paper.

Data availability

Data will be made available on request.

Acknowledgements

We extend our gratitude to the guides of Las Güixas cave and Sandra Brunet, Alberto Zárate and Maria José Ezquerra for their invaluable assistance during the monitoring program, and to the Ayuntamiento de Villanúa for the financial support. Additionally, we would like to express our appreciation to the CHE (Confederación Hidrográfica del Ebro) for providing climatic data from the Villanúa, Canfranc and Izas weather stations. Reyes Giménez acknowledges the support of the iMove 2023 mobility grants funded by CSIC. Miguel Bartolome is supported by the HORIZON TMA MSCA Postdoctoral Fellowships - Global Fellowships 2022 MODKARST project (n° 101107943) funded by the European Commission.

Appendix A. Supplementary data

Supplementary data to this article can be found online at https://doi.org/10.1016/j.jenvman.2024.122285.

References

Acín, V.A., Ferrer, D.B., Curiel, P.B., Zueco, S.D., Gil, F.E., Hidalgo, J.C.G., García, D.G., Matauco, A.I.G. de, Albero, C.M., Mur, D.M., Romero, E.N., Ojeda, A.O., Fabre, M.S., Sánchez, M.Á.S., Notivoli, R.S., 2012. Sobre las precipitaciones de octubre de 2012 en el Pirineo aragonés, su respuesta hidrológica y la gestión de riesgos. Geographicalia, pp. 101–128. https://doi.org/10.26754/ojs_geoph/geoph.2012611093.

Ahmed, J.U., Talukder, N., Alam, S.R., Ahmed, A., Faroque, A., 2021. Rescue mission in the Tham Luang Nang. Non cave, Thailand, London. https://doi.org/10.4135/9781529758122.

Baker, A., Genty, D., 1998. Environmental pressures on conserving cave speleothems: effects of changing surface land use and increased cave tourism. J. Environ. Manag. 53, 165–175. https://doi.org/10.1006/jema.1998.0208.

Baldini, J., 2010. Cave Atmosphere Controls on Stalagmite Growth Rate and Palaeoclimate Records, vol. 336. Geological Society, London, Special Publications, pp. 283–294. https://doi.org/10.1144/SP336.15.

Bartolomé, M., Giménez, R., Pérez-Villar, G., Gisbert, M., et al., 2023. El potential de los sedimentos de la cueva del Ubriga (El Vallecillo, Teruel) para la reconstrucción de paleoinundaciones. La Cija de Teruel 18, 15–19.

Bartolomé, M., Luetscher, M., Stoll, H., Moreno, A., Benito, G., 2024. Extreme flood events in the western Mediterranean: integrating numerical MODelling and flood records in KARST systems (MODKARST project). Geogaceta 75, 95–98. doi: 10.55407/geogaceta10099.

Bourges, F., Genthon, P., Mangin, A., D'Hulst, D., 2006. Microclimates of l'Aven d'Orgnac and other French limestone caves (chauvet, esparros, marsoulas). Int. J. Climatol. 26, 1651–1670. https://doi.org/10.1002/joc.1327.

Bourges, F., Genty, D., Perrier, F., Lartiges, B., Régnier, É., François, A., Leplat, J., Touron, S., Bousta, F., Massault, M., Delmotte, M., Dumoulin, J.-P., Girault, F., Ramonet, M., Chauveau, C., Rodrigues, P., 2020. Hydrogeological control on carbon dioxide input into the atmosphere of the Chauvet-Pont d'Arc cave. Sci. Total Environ. 716, 136844 https://doi.org/10.1016/j.scitotenv.2020.136844.

Breecker, D.O., Payne, A.E., Quade, J., Banner, J.L., Ball, C.E., Meyer, K.W., Cowan, B.D., 2012. The sources and sinks of CO2 in caves under mixed woodland and grassland vegetation. Geochem. Cosmochim. Acta 96, 230–246. https://doi.org/10.1016/j.gca.2012.08.023.

Chiarini, V., Duckeck, J., De Waele, J., 2022. A global perspective on sustainable show cave tourism. Geoheritage 14, 1–27. https://doi.org/10.1007/s12371-022-00717-5.

Cigna, A., 1993. Environmental management of tourist caves. Environ. Geol. 21, 173–180. https://doi.org/10.1007/BF00775302.

Cigna, A., Forti, P., 2013. Caves: the most important geotouristic feature in the world. Tourism and Karst Areas 6, 9–26.

Cigna, A.A., Burri, E., 2000. Development, Management and Economy of Show Caves. KIP Articles.

Constantin, S., Mirea, I.C., Petculescu, A., Arghir, R.A., Măntoiu, D. Ștefan, Kenesz, M., Robu, M., Moldovan, O.T., 2021. Monitoring human impact in show caves. A study of four Romanian caves. Sustainability 13, 1619. https://doi.org/10.3390/su13041619.

Crosson, E.R., 2008. A cavity ring-down analyzer for measuring atmospheric levels of methane, carbon dioxide, and water vapor. Appl. Phys. B 92, 403–408. https://doi.org/10.1007/s00340-008-3135-y.

Faimon, J., Troppová, D., Baldík, V., Novotný, R., 2012. Air circulation and its impact on microclimatic variables in the císařská cave (moravian karst, Czech republic). Int. J. Climatol. 32, 599–623. https://doi.org/10.1002/joc.2298.

Fernández-Cortés, A., Calaforra, J.M., Jiménez-Espinosa, R., Sánchez-Martos, F., 2006. Geostatistical spatiotemporal analysis of air temperature as an aid to delineating thermal stability zones in a potential show cave: implications for environmental management. J. Environ. Manag. 81, 371–383. https://doi.org/10.1016/j.jenvman.2005.11.011.

Fernandez-Cortes, A., Cuezva, S., Sanchez-Moral, S., Cañaveras, J., Porca, E., Jurado, V., Martin-Sanchez, P., Saiz-Jimenez, C., 2011. Detection of human-induced environmental disturbances in a show cave. Environ. Sci. Pollut. Res. Int. 18, 1037–1045. https://doi.org/10.1007/s11356-011-0513-5.

Gázquez, F., Quindós-Poncela, L., Sainz-Fernández, C., Fernández-Villar, A., Fuente-Merino, I., Celaya-Gonzalez, S., 2016. Spatiotemporal distribution of δ13CCO2 in a shallow cave and its potential use as indicator of anthropic pressure. J. Environ. Manag. 180, 421–432. https://doi.org/10.1016/j.jenvman.2016.05.078.

Giménez, R., Bartolomé, M., Gázquez, F., Iglesias, M., Moreno, A., 2021. Underlying climate controls in triple oxygen (16 O, 17 O, 18 O) and hydrogen (1 H, 2 H) isotopes composition of rainfall (central Pyrenees). Front. Earth Sci. 9, 209. https://doi.org/10.3389/feart.2021.633698.

Guirado, E., Gázquez, F., Fernandez-Cortes, A., Argumosa, A., Calaforra, J., 2015. Calculating the maximum visitability in tourist caves by CAVIX method: El Soplao (Cantabria, Spain) - Cálculo de la visitabilidad máxima en cavidades turísticas mediante el método CAVIX: El Soplao (Cantabria, España). Pesquisas em Turismo e Paisagens Cársticas 8, 38–43.

Heaton, T., 1986. Caves; a tremendous range of energy environments on Earth. Nat. Speleol. Soc. News August, 301–304.

Heeb, B., 2014. The next generation of the DistoX cave surveying instrument. CREG Journal 88, 5–8.

Holcomb, G.S., 2016. Temporal CO2 variations and the influence of bat colonies in speleogenesis: continuous CO2 monitoring in war eagle cavern, Arkansas. Graduate Theses and Dissertations. Retrieved from. https://scholarworks.uark.edu/etd/1782.

IPCC, 2021. In: Masson-Delmotte, V., Zhai, P., Pirani, A., Connors, S.L., Péan, C., Berger, S., Caud, N., Chen, Y., Goldfarb, L., Gomis, M.I., Huang, M., Leitzell, K., Lonnoy, E., Matthews, J.B.R., Maycock, T.K., Waterfield, T., Yelekçi, O., Yu, R., Zhou, B. (Eds.), Climate Change 2021: the Physical Science Basis. Contribution of Working Group I to the Sixth Assessment Report of the Intergovernmental Panel on Climate Change. Cambridge University Press, Cambridge, United Kingdom and New York, NY, USA. https://doi.org/10.1017/9781009157896 (in press).

Jakucs, L., 1959. Neue Methoden der Hohlenforschung in Ungarn und ihre Ergebnisse. Hohle 10 (4), 88–98.

Jeannin, P.-Y., 2001. Modeling flow in phreatic and epiphreatic Karst conduits in the Hölloch Cave (Muotatal, Switzerland). Water Resources Research 37, 191–200. https://doi.org/10.1029/2000WR900257.

Jeannin, P.-Y., Malard, A., 2018. A way to predict natural hazards in karst. Sinkhole Conference 2018.

Lang, M., Faimon, J., Pracný, P., Štelcl, J., Kejíková, S., Hebelka, J., 2024. Impact of water exhaled out by visitors in show caves: a case study from the Moravian Karst (Czech Republic). Environ. Sci. Pollut. Res. 31, 27117–27135. https://doi.org/10.1007/s11356-024-32946-2.

Li, Y., Yang, Y., Wang, X., Luo, W., Zhao, J., Sun, Z., Ye, Z., Chen, X., Shi, X., Xu, Y., Baker, J.L., 2024. Sources and transport of CO2 in the karst system of jiguan cave,

funiu mountains, China. Sci. Total Environ. 918, 170507 https://doi.org/10.1016/j.scitotenv.2024.170507.
Llasat, M.C., 2021. Floods evolution in the Mediterranean region in a context of climate and environmental change. Cuadernos de Investigación Geográfica 47, 13–32. https://doi.org/10.18172/cig.4897.
López-Moreno, J.I., Goyette, S., Beniston, M., 2008. Climate change prediction over complex areas: spatial variability of uncertainties and predictions over the Pyrenees from a set of regional climate models. Int. J. Climatol. 28, 1535–1550. https://doi.org/10.1002/joc.1645.
Lorenzo, J.I., 1992. LORENZO LIZALDE, José Ignacio (1992). Excavación en la cueva sepulcral de Las Guixas de Villanúa (Huesca). Arqueología Aragonesa 1990. Diputación General de Aragón, Zaragoza, pp. 359–363.
Mandić, M., Mihevc, A., Leis, A., Bronić, I.K., 2013. Concentration and stable carbon isotopic composition of CO_2 in cave air of Postojnska jama. Slovenia. International Journal of Speleology 42. https://doi.org/10.5038/1827-806X.42.3.11.
Mattey, D.P., Atkinson, T.C., Barker, J.A., Fisher, R., Latin, J.-P., Durrell, R., Ainsworth, M., 2016. Carbon dioxide, ground air and carbon cycling in Gibraltar karst. Geochem. Cosmochim. Acta 184, 88–113. https://doi.org/10.1016/j.gca.2016.01.041.
Mattey, D.P., Atkinson, T.C., Hoffmann, D.L., Boyd, M., Ainsworth, M., Durell, R., Latin, J.-P., 2021. External controls on CO2 in Gibraltar cave air and ground air: implications for interpretation of δ13C in speleothems. Sci. Total Environ. 777, 146096 https://doi.org/10.1016/j.scitotenv.2021.146096.
Nicolas, H., Lastennet, R., Denis, A., Malaurent, P., Minvielle, S., Peyraube, N., 2017. Assessing cave internal aerology in understanding carbon dioxide (CO2) dynamics: implications on calcite mass variation on the wall of Lascaux Cave (France). Environ. Earth Sci. 76, 170. https://doi.org/10.1007/s12665-017-6498-8.
O'Leary, M.H., 1981. Carbon isotope fractionation in plants. Phytochemistry 20, 553–567. https://doi.org/10.1016/0031-9422(81)85134-5.
OPCC-CTP, 2018. El cambio climático en los Pirineos: impactos, vulnerabilidades y adaptación. In: Bases de conocimiento para la futura estrategia de adaptación al cambio climático en los Pirineos, vol. 149.
Pérez-Zanón, N., Sigró, J., Ashcroft, L., 2017. Temperature and precipitation regional climate series over the central Pyrenees during 1910–2013. Int. J. Climatol. 37, 1922–1937. https://doi.org/10.1002/joc.4823.
Rivas, A., Cabezas, J., Carrasco, F., Durán, J.J., González-Ríos, M., 2004. Las cuevas turísticas españolas: un recurso natural de gran interés ecológico, económico y social. Andreo, B. y Durán, J. J. Investigaciones en sistemas kársticos españoles. Publicaciones del Instituto Geológico y Minero de España. Serie Hidrogeología y Aguas Subterráneas 12, 367–384.
Rodanés, J.M., Lorenzo, J.I., Aranda, P., 2016. Enterramientos en cuevas y abrigos en el Alto Aragón durante el Neolítico y la Edad del Bronce. Del neolític a l'edat del bronze en el Mediterrani occidental. Estudis en homenatge a Bernat Martí Oliver, Serie Trabajos Varios S.I.P. 119, pp. 411–426. València.
Serrano-Muela, M.P., Nadal-Romero, E., Lana-Renault, N., González-Hidalgo, J.C., López-Moreno, J.I., Beguería, S., Sanjuan, Y., García-Ruiz, J.M., 2013. An exceptional rainfall event in the central western Pyrenees: spatial patterns in discharge and impact. Land Degrad. Dev. 26, 249–262. https://doi.org/10.1002/ldr.2221.
Spötl, C., Fairchild, I.J., Tooth, A.F., 2005. Cave air control on dripwater geochemistry, Obir Caves (Austria): implications for speleothem deposition in dynamically ventilated caves. Geochem. Cosmochim. Acta 69, 2451–2468. https://doi.org/10.1016/j.gca.2004.12.009.
Thornwaite, C.W., 1954. The Measurement of Potential Evapotranspiration: Seabrook. John P. Mather, New Jersey, p. 225.
Tramblay, Y., Arnaud, P., Artigue, G., Lang, M., Paquet, E., Neppel, L., Sauquet, E., 2023. Changes in Mediterranean flood processes and seasonality. Hydrol. Earth Syst. Sci. 27, 2973–2987. https://doi.org/10.5194/hess-27-2973-2023.
Troester, J.W., White, W.B., 1984. Seasonal fluctuations in the carbon dioxide partial pressure in a cave atmosphere. Water Resour. Res. 20, 153–156. https://doi.org/10.1029/WR020i001p00153.
Vuilleumier, C., Jeannin, P.-Y., Perrochet, P., 2019. Physics-based fine-scale numerical model of a karst system (Milandre Cave, Switzerland). Hydrogeol J 27, 2347–2363. https://doi.org/10.1007/s10040-019-02006-y.
Worthington, S.R.H., 1994. Flow velocities in unconfined carbonate aquifers. Cave Karst Sci. 21 (1), 21–22.